SCIENCE CHINA
Earth Sciences

SPECIAL TOPIC: China since the Last Glacial Maximum
•RESEARCH PAPER•

August 2019 Vol.62 No.8: 1207–1223
https://doi.org/10.1007/s11430-018-9272-0

Evolution of permafrost in China during the last 20 ka

Huijun JIN[1,2,3*], Xiaoying JIN[1,3†], Ruixia HE[1], Dongliang LUO[1‡], Xiaoli CHANG[1,4], Shaoling WANG[1], Sergey S MARCHENKO[1,5], Sizhong YANG[1,6], Chaolu YI[7], Shijie LI[8] & Stuart A HARRIS[9]

[1]*Northeast China Observational Station of Cold-regions Engineering and Environment, State Key Laboratory of Frozen Soils Engineering, Northwest Institute of Eco-Environment and Resources, Chinese Academy of Sciences, Lanzhou 730000, China;*
[2]*School of Civil Engineering, Harbin Institute of Technology, Harbin 150090, China;*
[3]*School of Resources and Environment, University of Chinese Academy of Science, Beijing 100049, China;*
[4]*Hunan University of Science and Technology, Xiangtan 411201, China;*
[5]*Permafrost Laboratory, Geophysical Institute, University of Alaska Fairbanks, Fairbanks, AK 99775, USA;*
[6]*GFZ German Research Centre for Geosciences, Telegrafenberg, Potsdam D-14473, Germany;*
[7]*Institute of Tibetan Plateau Research, Chinese Academy of Sciences, Beijing 100010, China;*
[8]*Institute of Geochemistry, Chinese Academy of Sciences, Guiyang 550081, China;*
[9] *Department of Geography, University of Calgary, Calgary, Alberta T2N 1N4, Canada*

Received January 26, 2018; revised June 21, 2018; accepted September 14, 2018; published online November 29, 2018

Abstract The formation and evolution of permafrost in China during the last 20 ka were reconstructed on the basis of large amount of paleo-permafrost remains and paleo-periglacial evidence, as well as paleo-glacial landforms, paleo-flora and paleofauna records. The results indicate that, during the local Last Glacial Maximum (LLGM) or local Last Permafrost Maximum (LLPMax), the extent of permafrost of China reached 5.3×10^6–5.4×10^6 km^2, or thrice that of today, but permafrost shrank to only 0.80×10^6–0.85×10^6 km^2, or 50% that of present, during the local Holocene Megathermal Period (LHMP), or the local Last Permafrost Minimum (LLPMin). On the basis of the dating of periglacial remains and their distributive features, the extent of permafrost in China was delineated for the two periods of LLGM (LLPMax) and LHMP (LLPMin), and the evolution of permafrost in China was divided into seven periods as follows: (1) LLGM in Late Pleistocene (ca. 20000 to 13000–10800 a BP) with extensive evidence for the presence of intensive ice-wedge expansion for outlining its LLPMax extent; (2) A period of dramatically changing climate during the early Holocene (10800 to 8500–7000 a BP) when permafrost remained relatively stable but with a general trend of shrinking areal extent; (3) The LHMP in the Mid-Holocene (8500–7000 to 4000–3000 a BP) when permafrost degraded intensively and extensively, and shrank to the LLPMin; (4) Neoglaciation during the late Holocene (4000–3000 to 1000 a BP, when permafrost again expanded; (5) Medieval Warming Period (MWP) in the late Holocene (1000–500 a BP) when permafrost was in a relative decline; (6) Little Ice Age (LIA) in the late Holocene (500–100 a BP), when permafrost relatively expanded, and; (7) Recent warming (during the 20th century), when permafrost continuously degraded and still is degrading. The paleo-climate, geography and paleopermafrost extents and other features were reconstructed for each of these seven periods.

Keywords Permafrost evolution, Cryogenic wedge structures, Local Last Glacial Maximum (LLGM), Local Holocene Megathermal Period (LHMP), China

Citation: Jin H, Jin X, He R, Luo D, Chang X, Wang S, Marchenko S S, Yang S, Yi C, Li S, Harris S A. 2019. Evolution of permafrost in China during the last 20 ka. Science China Earth Sciences, 62: 1207–1223, https://doi.org/10.1007/s11430-018-9272-0

* Corresponding author (email: hjjin@lzb.ac.cn)
† Corresponding author (email: lncyjxy@163.com)
‡ Equal contribution (email: luodongliang@lzb.ac.cn)

1. Introduction

In China, the local Last Glacial Maximum (LLGM, 26−16 ka BP) was the coldest period and the local Holocene Megathermal Period (LHMP, 8.5−7 to 4−3 ka BP) was the warmest period since the end of the Late Pleistocene (Shi, 1998, 2006, 2011; Zheng et al., 1998; Shi et al., 2000). During these two periods, climate fluctuations, in different cold-warm and dry-wet combinations, directly controlled the distribution of glaciers and permafrost and their changes. Therefore, understanding the past and present distribution, degradation rates, shrinking areal extents and volumes of permafrost is key to studying the source and sink effects of climate change and permafrost dynamics on the carbon pools in the atmosphere, soil and shallow permafrost.

Although the Last Glaciation Maximum (LGM) was the latest glaciation period, there was no a unified ice sheet, and snow and ice coverage was limited on the Qinghai-Tibet Plateau (QTP) and its peripheral mountains (Shi et al., 1990, 1995; Zheng, 1990; Shi, 2006, 2011; Heyman, 2010). Permafrost may have intensively developed, extensively expanded and reached the local Last Permafrost Maximum (LLPMax), establishing the framework of existing permafrost in China (Zhao et al., 2013). Later, it underwent the local Last Permafrost Minimum (LLPMin) in the local Holocene Megathermal Period (LHMP) and a series of evolutionary processes, forming the present distributive features of permafrost in China (Zhou et al., 1991; Qiu and Cheng, 1995; Zhou et al., 2000; Jin et al., 2007a, 2016; Chang et al., 2017).

At present, the areal extent of permafrost in China is 1.59×10^6 km^2, including an areal extent of plateau permafrost at 1.05×10^6 km^2 on the QTP, an areal extent of latitudinal permafrost at 0.24×10^6 km^2 in Northeast China, and an areal extent of mountain permafrost at 0.30×10^6 km^2 mainly in West and Central China (Ran et al., 2012). The areal extent of seasonally frozen ground in China at present is 5.36×10^6 km^2, mainly found in North and Central China. In addition, at the beginning of the last 20 ka, permafrost may have occurred in most regions in Northwest, North, and Northeast China and on the Qinghai-Tibet Plateau. Rising sea levels permitted the East Asian Monsoon to re-develop, resulting in a change from very cold, dry conditions to warmer, more humid conditions marked by the rise and decline of ice-wedges, leaving behind a large amount of evidence and landscapes of Quaternary permafrost and periglacial phenomena. In this paper, the evolution processes and distributive features of permafrost in China since the last 20 ka were reconstructed on the basis of clarifying and using those numerous reported and recently identified evidence and proxies for inferring the past permafrost and periglacial environment. This study aims at providing a basic understanding and key scientific baseline for rebuilding the cold regions environment and carbon turnovers and their change rates among the glacial and interglacial periods in China and beyond.

2. Study methods

2.1 Research method for Quaternary paleo-permafrost

Under the dry cold conditions at ca. 20–21 ka BP, there was negligible water supply so that ice-wedges could not form. With the onset of the East Asian Monsoon due to rising sea levels, the warm precipitation entered the soil, producing ice wedges and bodies of ice. The heat, brought with the precipitation, plus the heat emitted during crystallization, resulted in warming the surrounding permafrost. The resulting ground ice is the evidence for past permafrost and paleo-periglacial geomorphology. However, this evidence is often subject to various interpretations (e.g., Vandenberghe, 1992; Vandenberghe and Pissart, 1993; Murton and Kolstrup, 2003; Harris et al., 2017; French, 2018). The formation, development, areal extent and evolution of past permafrost are estimated and reconstructed on the basis of Quaternary geology and paleo-biology, -climatology and -environmental proxies and data, and related dating techniques, under the principle of "the present as the key to the past", often aided by numerical model reconstruction (e.g., Liu et al., 2002; Jiao et al., 2015, 2016).

2.2 Evidence and criteria for past permafrost

The evidence for the occurrence of permafrost can be classified into two categories: direct and indirect indicators. Direct indicators include primary and secondary wedge structures, deeply buried permafrost and massive ground ice, past permafrost tables, pingos and pingo scars, lithalsas and palsas, to just name a few. Indirect indicators can be cryoturbations or cryogenic involutions, soil wedges and cryogenic polygonal structures, active or paleo-rock glaciers (e.g., Schmid et al., 2015); sorted and patterned ground, block fields, as well as pollen records in soil strata, such as *Picea* and *Abies* or other indicators of cold floristic communities, paleosols; glacial tills and landforms; periglacial flora and fauna (such as mammoths, wooly rhinos, and hardy plants), and characteristic combinations of clay minerals in soil strata. Some of these indicators are subject to multifaceted interpretations. Reliable conclusions can only be reached by comprehensive studies using multi-proxy combinations and cross-examinations.

The response of permafrost to climate change has a substantial time lag. On the ground surface, the relics of previous permafrost stages are often buried or erased by the next or new evolution events, only to increase the challenges for reconstructing a more detailed sequence of permafrost evo-

lution. In another word, the closer to the present, the richer and more detailed the identified relics of permafrost. Therefore, various permafrost relics since the last 20 ka have been relatively better preserved. In recent decades, continuous and rapid advancement in sediment dating, more sophisticated and accurate dating methods, and continuous enrichment of various experimental and geoscience data have enabled more systematic approach and methods, and have resulted in more reliable results. In order to draw better conclusions in the formation and development of the permafrost environment, it is necessary to combine and validate with the results from Quaternary glaciology, desert research, periglacial studies, and paleo-climatology, -geography and -environment. These processes can largely overcome the multiplicity in the interpretations for some periglacial phenomena and eliminate as possible the false understanding.

The estimation of paleo-ground-temperature is important in understanding the occurrence and developmental conditions of past permafrost. It can be achived by using the paleo-air-temperatures, or interpretations from various paleo-cryogenic wedge structures. On the basis of field observations and lab experiments, Romanovskii (1977) summarized and pointed out that cryogeneic wedge structures, such as soil/ground, sand and ice wedges, as well as ice-wedge pseudomorphs (casts) resulting from cryogenic polygonal cracking, were closely related to the properties of soil sediments, soil moisture contents, and ground temperatures. The finer the soil grains, the lower the temperatures for the formation of cryogenic wedge structures. To grow soil wedges in fine-grained soils, such as fine sands, silts, sandy loams, clay, peat and humic soils, a mean annual ground temperature (MAGT) of −2 to −1°C, or lower, is needed, whereas those in the coarse-grained soils, such as medium and coarse sands and sandy gravels, would need an MAGT of −5 to −3°C, or lower, while ice wedges in coarse soils would mandate an MAGT of −6 to −5°C or lower. Up to date, this method of using cryogenic wedge structures for inferring paleo-temperatures have been widely adopted as a traditional method in rebuilding the Quaternary permafrost environment in China (e.g., Cui, 1980; Liang and Cheng, 1984; Pan and Chen, 1997; Cui et al., 2002, 2004; Jin et al., 2007a, 2011a, 2011b, 2016; Chang et al., 2011, 2017), and beyond (e.g., Harris et al., 2017; French, 2018).

3. Statistics on paleo-permafrost and criteria for southern/lower limit of permafrost

3.1 Statistics on paleo-permafrost

The ages for the formation and thawing of paleo-permafrost are key in statistics and analyses of various paleo-permafrost relics and data. The authors of this paper have extensively collected, verified and extended the dating data on the basis of Quaternary glacial periods in China provided by Shi (2006), in addition to the statistics of related age data for past permafrost in China (see Appendix 1, available at http:earth.scichina.com). These data serve as the baseline for the divisions of chronological sequences of permafrost evolution in China. They were further elaborated with several representative profiles of wedge structures and some photos of typical cryogenic structures (Figure 1).

3.2 Delineation of paleo-permafrost boundaries

Paleo-permafrost remains, e.g., ice wedge pseudomorphs (casts) and rock, sand, soil and primary ice wedges in particular, are key indicators for reconstruction the paleo-environment and Quaternary boundaries of permafrost. Large numbers of wedge structures with various shapes and geneses have been identified. They can only be indicative of paleo-permafrost when they are clarified and verified as groups of cryogenic sand, soil and rock wedges closely related to frost cracking polygons and permafrost. By using the relationships of wedges to the host strata, ice wedges and ice wedge pseudomorphs (casts), and sand, soil and rock wedges can be recognized. Ground temperatures for the formation of wedge structures are related to wedge structure types and soil strata. Due to rapid tectonic uplifts in recent geohistory, it is necessary to make elevational and latitudinal adjustments for estimated air or ground temperatures: 6°C km^{-1} (elevation) and 1°C $°N^{-1}$ (Zhou et al., 2000).

Since the Late Peistocene, the QTP has been uplified by about 1000 m. Due the short time period involved in this discussion, an elevation of 500 m, as justified in Zhou (2007), is assumed in this paper. In addition, the adjustments have to take into account the tectonic units of these identified cryogenic structures, such as those of the Tianshui'hai Lake region in the relative uplift zone in the West Kunlun Mountains, and Nachitai along the Qinghai-Tibet Highway (QTH) in the Eastern Kunlun Mountains, the Gong'he Basin on northeastern QTP, and the Lenghu Basin on northern QTP in the relative subsidence zone. The southern/lower limit of permafrost (SLP/LLP) and distributive features, as well as paleo-geography, can then be delineated on the basis of adjusted air or ground temperatures.

4. Results and discussions

Many paleo-permafrost and paleo-periglacial remains of different ages since the Middle Pleistocene have been identified in China (e.g., Pan and Chen, 1997; Zhou et al., 2008; Qi et al., 2014). However, the main body of the existing permafrost in China was formed during the LLGM in the Late Pleistocene (Zhou et al., 1965, 2000; Zhao et al., 2013; Jin et al., 2016; Chang et al., 2017). Since the Late Glacial

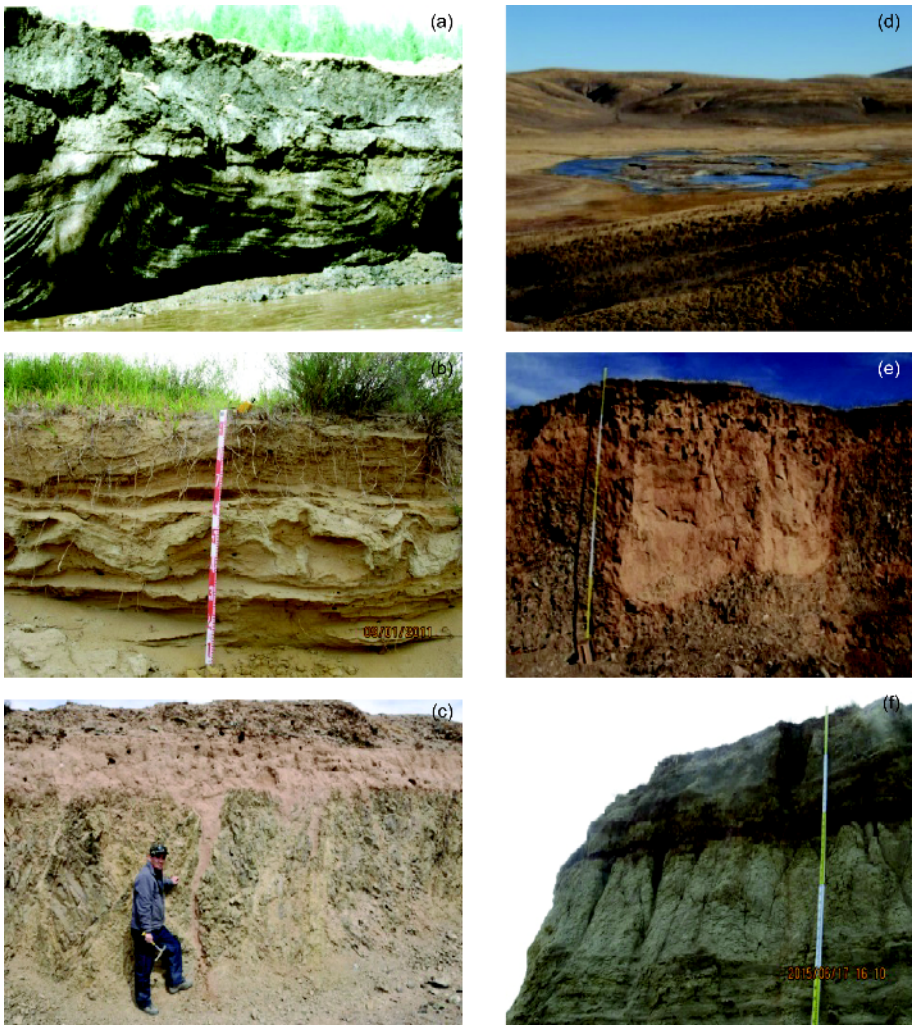

Figure 1 Photos of typical cryogenic structures in China (only 6 sites are listed). (a) Ice wedges in Wuma, northern Da Xing'anling Mts. (b) Cryoturbations in Dishaogou Valley, Salawusu, Inner Mongolia. cryoturbations in yellowish fine sand with grayish silts. (c) Sand wedges in Huang'he Village, Madoi, Qinghai. (d) Pingo plateau northwest of the Ngöring Lake, SAYR. (e) Cryoturbations on the first terrace of the Datong River near Huangchengzi, Menyuan, Qinghai: 150 m×5 m, location at 37°38′25.2″N, 101°9′43.3″E; 3148 m asl. (f) Frost-cracking sand wedges at Yixing Logistics Co. in Dongsheng, Ordos, Inner Mongolia.

period in the early Holocene, permafrost has undergone many expansions and retreats, forming the present patterns of distribution of permafrost in China.

Taking into account lagged responses of permafrost to climate changes, the LLPMax occurred about 20 ka BP. Later, many major climatic and environmental changes, such as the LLGM and LHMP, have reshaped the distributive features of permafrost (Zheng et al., 1998). The LLPMax and LLPMin in China also took place (Figure 2) (Zhao et al., 2013; Harris et al., 2016; Jin et al., 2016; Chang et al., 2017).

Permafrost evolution in China since 20 ka BP can provisionally be divided into seven major periods on the basis of the distribution of existing permafrost in China and analyses of spatiotemporal differentiations of paleo-permafrost and -periglacial remains listed in the Appendix 1, in addition to cross-correlations with Quaternary glacial, paleo-climatic and -environmental records. Among them, the LLGM/LLPMax and LHMP/LLPMin are the most important periods for the development, growth and evolution, as well as the distribution of the existing permafrost in China. In those above-mentioned seven periods, some sub-tier changes in climate, permafrost and periglacial environments occurred. However, the responses of permafrost to these second-tier changes have been overlapped or erased by these seven major climatic climaxes (the coldest or warmest). Therefore, under these complex circumstances, only distribution of permafrost under those longer-term climate extremes, i.e., the maxima or minima of permafrost extent, can be rebuilt.

On the studies and integration of paleo-permafrost in the periphery or bordering states and/or regions, an attempt is made for merging the reconstruction of LLGM permafrost in China with some other regions (Figure 2). It seems that the boundaries of permafrost in China merge with those in Kazakhstan, Central Asian states, and western Asia. However, it

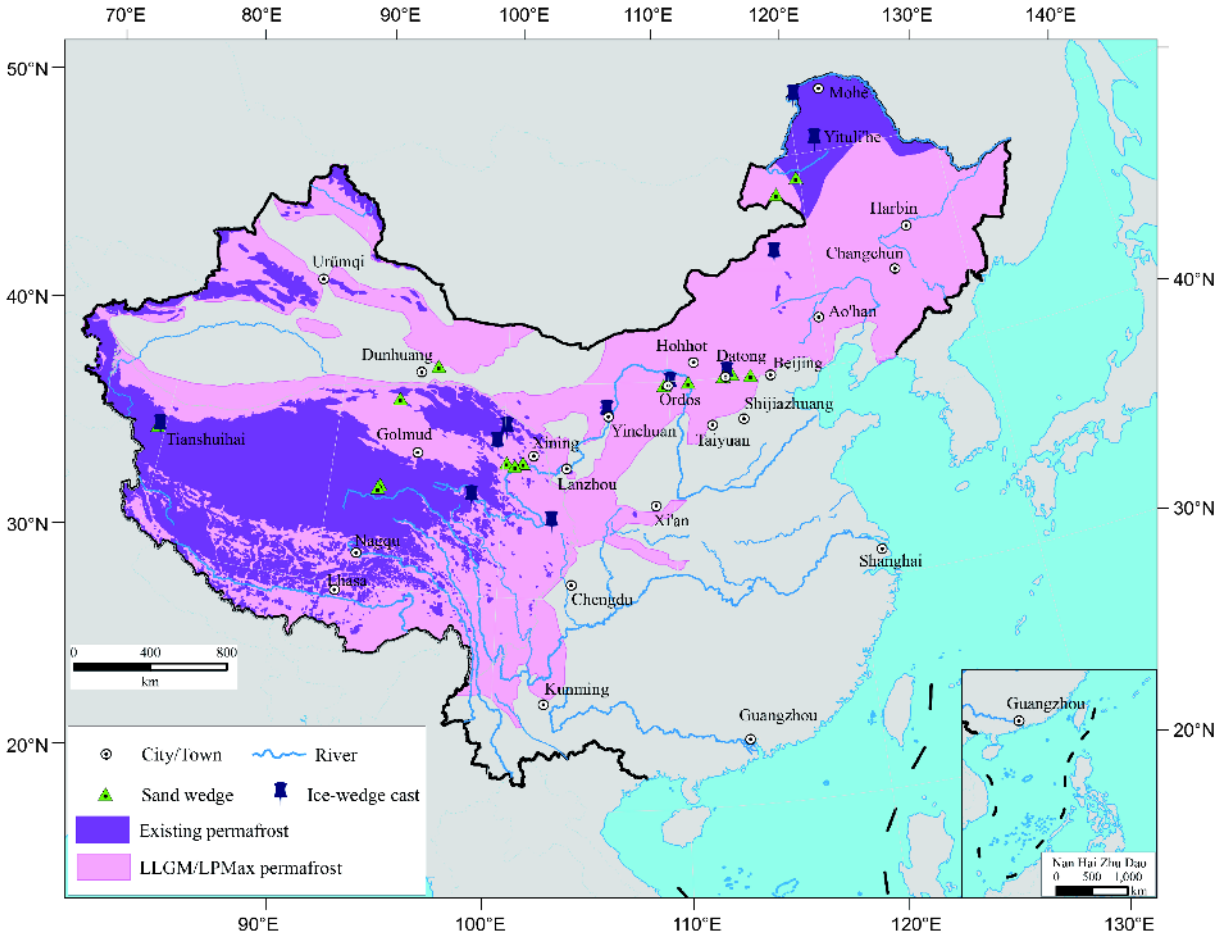

Figure 2 Distribution of permafrost in China during the LLPMax/LLGM and at present.

still needs data from Russia, Mongolia and Korean Peninsula to integrate the paleo-permafrost map with Eurasian permafrost body during the LLGM. In the meantime, it should be pointed out that due to large amplitudes of sea level drop amounting as 120−150 m during the LLGM, the general circulations and distribution of land-ocean, as well as some major landscapes and vegetation, were affected, complicating the reconstruction of paleo-permafrost in China and bording states. In particular, these mosaicked distributions of permafrost and talik in deserts have been discussed, but still lack reliable evidence for mapping these regions.

4.1 Permafrost during the LLPMax in the end of the Late Pleistocene (LLGM, ca. 20 to 13−10.8 ka BP): permafrost was extremely well developed

The climax of LGM (26−16 ka BP) witnessed the latest large-scale glaciations, with a massive cooling in the Northern Hemisphere (Shi, 1998; Shi et al.,1990, 1995, 1997; Zheng, 1990; Wang and Sun, 1994; Zheng et al., 1998). In the meantime, glaciations expanded in North China and on the QTP; however, the spatial scales of glaciations were limited on the QTP and in its periphery mountains, and mountains in Central Asia, and Northeast, North and Central China (Sun et al., 1985; Li et al., 1991; Shi et al., 2000; Shi, 2006; Heyman, 2010). Therefore, it could have been the LLPMin in China. Many paleo-permafrost and -perlglacial remains have been well and extensively preserved (Appendix 1). In particular, large numbers of cryogenic wedge structures, especially those extensively identified sand and soil wedge groups, formed during the LLGM, have been found in China. In addition, numerous cryogenic wedge structures have also been discovered and archived in most regions of what is seasonally frozen ground at present, such as the Ordos (Loess) Plateau, QTP, North China and southern part of Northeast China (e.g., Zhang, 1983; Xu and Pan, 1990; Wang and Bian, 1993; Pan and Chen, 1997; Cui et al., 2004, 2004; Vandenberghe et al., 2004, 2016; Cheng et al., 2006; Jin et al., 2006a, 2006b, 2007a, 2016; Zhou, 2007; Zhou et al., 2008; Chang et al., 2011, 2017; Harris and Jin, 2012; Wang et al., 2013; Xu et al., 2015; Harris et al., 2016, 2018). These wedges were generally formed at the margins of lacustrine or river terraces, and covered by sediments of 1−2 m in thicknesses. In profiles of some of those wedge

structures, falling textures and blocky and gravelly infills can be identified, which can be related to the melting of ground ice.

A very cold and dry climate prevailed on the QTP during the LLGM until 14 ka BP. Afterwards, climate warmed up intermitently, and the growth of some wedges stopped due to the rising air temperatures. According to the ice-core records from the Gulia Ice Cap in the West Kunlun Mountains, a warming of about 2−3°C occurred during 14−12 ka BP, although there were still appreciable ups and downs in air temperatures (Shi, 2011). By the end of the Late Peistocene, the major distribution patterns of existing permafrost on the QTP were already established (Jin et al., 2007a; Chang et al., 2017).

On the basis of the interpretations for numerous wedge structures, mean annual air temperatures (MAAT) were about 7−9°C colder than today on the QTP at ca. 20 ka BP (Jin et al., 2007a; Chang et al., 2017). Shi et al. (1995, 2000) concluded that, on middle and eastern QTP, it was 6.8°C colder than today. On the Zoîgé Peat Plateau, it was 5.8−7.9 °C cooler, as inferred from an 1200-m lowering of the upper timberline. Based on pollen records, the deduced paleotemperatures at the LLGM were about 6−7°C cold than today (Shen et al., 1996). On the basis of paleo-periglacial landforms, Cui (1980) estimated an MAAT 5.5−6.4°C cooler than today for the Tanggula Mountains in the Interior of the QTP. By comparing the changes in the lower limits of paleopermafrost, Yang and Wang (1983) estimated MAAT's (a cooling of) about 5−6°C colder than today for the plateau regions south of the Tanggula Mountains. Zheng (1990) believed that because of the large areal extent and massive relief of the QTP, there should be a marked differentiation in climate cooling during the LLGM with a decrease in MAAT of 5−7°C in the Interior and alpine regions of the QTP, 8−10°C in the peripheries. On the basis of surface pollen records in Rencuo, Basu County, Tibet Autonomous Region, Tang et al. (1998) deduced that the mean January air temperature at ca. 18 ka BP was 10°C lower than today, i.e. a cooling of about 6°C. On the basis of large cryoturbations and glaciofluvial sediments in Menyuan, Qinghai Province, Wang et al. (2013) estimated an MAAT during the LLGM at least 7°C colder than today, resulting in glaciers advancing to the foothills of the Qilian Mountains. Vandenberghe et al. (2016) and Harris et al. (2016) also have similar notions.

Reconstruction using numerical climate modeling reconstruction for the QTP indicates an MAAT for the LLGM of 2−13°C (Liu et al., 2002), 6°C (Böhner and Lehmkuhl, 2005), and 1.8−6.4°C, colder than today (Ju et al., 2007). Mark et al. (2005) estimated a reduction of MAAT of 7.5°C on the QTP according the changes in snowline, or the equilibrium line altitude (ELA). In a word, most scholars more or less have reached similar conclusions on the LLGM magnitude of the cooler air temperatures on the QTP. Thus, it is reasonable to assume an LLGM cooling of 7−9°C. However, Heyman (2010) and Owen et al. (2003, 2006) suggested that the glacial expansion was very limited on the basis of their latest studies on the QTP and adjacent regions with an MAAT only 2−4°C colder than today. There was no unified QTP or regional icesheet; most of plateau glaciers were formed long time ago and with ony limited expansions during the LLGM (Heyman et al., 2008, 2009; Stroeven et al., 2009).

Groups of inactive ice wedges were also found in Wuma (52°45′N, 120°45′E), northwestern corner of the Da Xing'anling Mountains, Northeast China (Tong, 1993). On the basis of AMS-^{14}C dating of ambient and overburden soils of the ice wedges, they were formed during 14475 ±304−10668±257 a BP. It would need a reduction of MAAT of about −7 to −5°C for forming ice wedges in the sandy soils (Romanovskii, 1977). The observations indicate that the present MAGT is 3.8−4.3°C higher than the MAAT in the northern Da Xing'anling Mountains (Chang et al., 2015; Jin et al., 2016). It is estimated that, when these ice wedges were formed, the local paleo-MAAT was about −10 to −9°C (Tong, 1993). The present-day MAAT in this region was about −5°C (in the 1990s), so that the northern Da Xing'anling Mountains were about 4−5°C colder during the period of ice-wedge growth period than today (Jin et al., 2016). To the south in the middle-western part of Northeast China, the Hulun Buir High Plain was sparsely vegetated under a dry continental climate during 22−11 ka BP (Yang et al., 2006).

In the arid regions in North China, Yu et al. (2013) rebuilt the paleoclimate during the LLGM (ca. 26−16 ka BP) on the basis of a large amount of paleodata, with a climatic cooling of about 5−11°C and a variability (uncertainty) of 60−200%; the concurrent decline in annual precipitation was about 180−350 mm. At the end of the Late Pleistocene, the present-day topography, geomorphology and topography were largely formed in the arid regions in Northeast and North China. Therefore, the SLP at the LLGM can be largely determined by the 0°C isotherms of MAAT (Jin et al., 2007b). In Northeast China, assuming an MAAT of 4−5°C colder than today and a northward cooling rate of 1°C/°N (Zhou et al., 2000), the SLP at the LLGM could have extended southwards by 4°−5°N, i.e., reaching 41°−42°N (Figure 2). The LLGM SLP and LLP met in the Liupanshan and Hua'jialing mountains on the Longdong Plateau (near Lanzhou) at elevations of 2200−2300 m asl (Zhou et al., 2000; Jin et al., 2007a, 2016; Zhao et al., 2013; Chang et al., 2017). This estimation was later confirmed by discoveries of many frost-cracked wedges on the Ordos (Loess) Plateau and it was concluded that the coldest paleoevironment in the LLGM of about 10−12°C colder than today occurred between 25−13 ka BP, when permafrost expanded southwards to south of 37°−38°N (Cui et al., 2004; Vandenberghe et al., 2004).

On the QTP and in the alpine regions in Central and West China, the MAAT at the LLP generally ranged from −4 to −2°C. There the LLP decreases by about 160−170 m for every 1°C cooling in MAAT (Wang and Bian, 1993). The LLP during the LLGM was 1200−1400 m lower than that of today, inferred from the combined evidence from the 7−9°C cooling of MAAT on the QTP and in alpine regions, the distribution of cryogenic wedge structures and other periglaical remains, and the lowering of the upper timberline (Jin et al., 2007a; Zhao et al., 2013; Chang et al., 2017). The plateau permafrost expanded and descended into the peripheral inland basins, such as Xinghai, Gong'he, Zoîgé, Chaidam and Tarim basins, with an areal extent of continuous permafrost at about 2.2×10^6 km^2. Sporadic and isolated patches of permafrost were also extensively distributed in mountainous areas in West China. Thus, the LLP could be estimated as follows:

(1) On western and northwestern QTP, the LLP was at 2800−2900 m above present-day sea level in western section of northern slopes of the West Kunlun Mountains, at 2400−2500 m asl on eastern section of northern slopes of the West Kunlun Mountains, and at 2900–3100 m asl in the southern margin of the Tarim Basin.

(2) On eastern QTP, the LLP was at 2300−2400 m asl in the Gong'he Basin, 2600−2800 m above present-day sea level in the Chaidam Basin, 2700−2800 m asl on the Zoîgé Plateau, 3000−3200 m asl on the Chuanxi (West Sichuan) Plateau, and 3800−4000 m asl in the Hengduan Mountains; on southern QTP, it was at 3600−3800 m asl in the middle- and down-streams of the Yarlong Zangpo River Basin in southern Tibet Autonomous Region.

(3) On northern QTP, the LLP was at 2200−2300 m above present-day sea level on northern slopes (Lenglongling Mountains) of Qilian Mountains and mountainous regions south of the Jiayuguan Pass, Gansu Province.

(4) The LLP was at 2100−2200 m asl on southern slopes and at 1900−2000 m above present-day sea level on northern slopes of the Chinese Tianshan Mountains, and 1400−1500 m asl on southern slopes of the Chinese Altai Mountains.

In summary, except for taliks in some deserts and lowland basins, the majority parts of North China and QTP were in permafrost zones (Figure 2), with a total permafrost extent at 5.3×10^6−5.4×10^6 km^2, or three times of the present permafrost extent.

During the LLGM, periglacial landforms were extensively developed, leaving behind many areas of relict permafrost, such as those primary sand wedges in medium and fine sands (Q_3 Gong'he Group sediments) on northeastern QTP reported by Xu (1984), Pan and Chen (1997), with a formation time prior to 20403±430−19430±360 a BP. Numerous sand wedges and ice wedge pseudomorphs have been identified and studies in the Source Area of the Yellow River with a formation age at 12300±100−16340±250 a BP (Pan and Chen, 1997; Cheng et al., 2006). The soil wedges in Nachitai on northern slopes of the Kunlun Mountains along the QTH were formed during 14041±339−15377±292 a BP; while the sand wedges in the Fenghuoshan Mountains in the Interior of the QTP were formed at 23500±1200 and 15340±770−9218±189 a BP. Sand wedges in Lenghu of the middle and northern parts of Qinghai Province were TL-dated at 18510±2220 a BP (Ma, 1996). Inactive ice wedges and primary sand wedges on the terrace of the Tianshuihai North Lake in the West Kunlun Mountains were formed during 21−12 ka BP (Li and He, 1990; Li and Jiao, 1990; Chang et al., 2011). In a 5-m-high roadcut close to Huangchengzi, Menyuan Hui Prefecture, Qinghai Province, on the southern flank of the Qilian Mountains, very large load castings developed after the OSL 20−30 ka BP (Vandenberghe et al., 2016; Harris et al., 2016).

Due to the extremely cold and dry continental climate, the plateau vegetation severely degraded during the LLGM. The majority of the plateau surface reverted to desert, steppe, or tundra environments: while lakes shrank and deserts expanded. Steppes extended eastwards to Linxia, Gansu Province and to the Zoîgé Plateau, Sichuan Province, and southwards to Basu County to the Yarlung Zangpo River Basin, southeastern Tibet Autonomous Region. Forests retreated to the eastern and southern edges of the QTP, with only some small patches of alpine shrublands and mountain needle- and broad-leaved mixed forests on the Western Sichuan and south of the Yarlung Zangpo River (Tang et al., 1998).

In Northeast China, a rich pollen assemblage of *Picea* and *Abies* have been found in the strata of the Guxiangtun Group in the Late Pleistocene in Huangshan, Harbin, Heilongjiang Province and Yushu County, Jilin Province, indicating a forest-steppe landscape. Based on incomplete statistics, fossils and remains of a Mammoth *(Mammuthus)*-Wooly Rhino (*Coelodonta*) fauna, an indicator for cold climate, have been excavated in many places in both the southern part of Northeast China and in the northern part of North China, concentrated in areas north of 42°N (Qiu, 1985; Zhang, 2009; Wei et al., 2010). By integrating the evidence from the extensive occurrences of the dark needle-leaved forests and Mammoth (*Mammuthus*)-Wooly Rhino (*Coelodonta*) fauna in these regions, it is evident that at the end of the Late Pleistocene, a cold climate prevailed in northern and mountainous parts of Northeast China, as well as the Songhuajiang-Liao'he Plain in Northeast China (Guo and Li, 1981), even in the lately exposed extensive continental shelves as a result of lowering sea level (Zhao et al., 2013; Jin et al., 2016). Since the 1970s, many megafauna, such as *Mogaloceros ordosianus* and *Mammuthus*, have been excavated in primary strata of the Late Pleistocene in the Bay of Bo'hai Sea. This at least can serve as concrete evidence for

cold climate in Northeast China.

Since coming into the Holocene, in comparison with the LLPMax/LLGM, the areal extent of permafrost was on a general decline. The history of permafrost evolution can still be divided into six distinct periods since the early Holocene starting at 10.8 ka BP.

4.2 Early Holocene with dramatic climate changes (10800 a BP to 8500−7000 a BP): period of stable but relatively shrinking permafrost

Unlike the LLPMax/LLGM, the areal extent of permafrost during the Holocene was on a general decline. The history of permafrost evolution can still be divided into six distinct periods since the early Holocene starting at 10.8 ka BP. The climate in the early Holocene was very unstable. A sharp cooling is indicated by the ice-core records from the Dunde Glacier, Qilian Mountains (38°06′N, 96°24′E; 5200 m asl): at 8700 a BP, with the $\delta^{18}O$ reaching −12.75‰, the lowest in the Holocene, whereas rose to −9.60‰ at 8500−8400 a BP, the highest in the Holocene, indicating a spike in climate warming (Yao and Shi, 1992). Accordingly, the diatom records in the Angren Co (Lake) in southern Tibet Autonomous Region indicate a lower lake temperature and a rising lake water salinity, i.e., a cold and dry period, prior to 8700 a BP (AMS-^{14}C), but during 8700−8600 a BP, the records suggest a very high lake temperature, with lowered lake water salinity and large input of glacier-melt (Li and Jiao, 1990).

The climate in early Holocene was cold and dry, but it was gradually changing to cool and moist climate. On the basis of the remains of paleo-permafrost, the northern LLP was at 3400−3500 m asl to the north of Nachitai along the QTH, the southern LLP was at 4200−4300 m asl between Yangjiajing and Damxung, northern Tibet Autonomous Region, while the LLP was about 600−700 m lower than today. Permafrost was continuous and thermally stable, but overall it was degrading from the LLPMax, with a declining areal extent of permafrost, although the permafrost extent was still 40−50% greater than today.

Song and Xia (1990) reported 150 pingo scars on the Sanjiang Plain (47°10′−48°43′N, 133°−135°E) in the northern part of Northeast China. They are generally accompanied by pingo-thawed lakes in round or oblong shapes, with a diameter of about 10−100 m. The outer margins of pingo scars generally have a wall of about 23 m in height, with an outlet. Generally, inside the walled lakes, water bodies can be found, or they have gradually developed into wetlands. Most of these pingo scars were formed during 10−8 ka BP (Li, 1990; Song and Xia, 1990). Therefore, it is evident that permafrost still occurred on the Sanjiang Plain in the early Holocene, but the permafrost to the south had largely vanished.

On the basis of pollen records from 20 lakes on the QTP, Tang and Shen (1996) synthesized the environmental features of the plateau in the early Holocene as follows. During ca. 10000−9100 a BP, mesophytic deciduous broad-leaved and needle-leaved forests dominated on eastern QTP. During ca. 10800−8000 a BP, *Artemisia* and *Chenopodiaceae* dominated in the subalpine steppe in the region of the Qinghai Lake on northeastern QTP, where there was an evident spike of arbor species pollens of more than 50% at 9500−8800 a BP, indicating a sudden warming and wetting (Du et al., 1989). During 10000−7700 a BP, *Artemisia* dominated the vegetation on the steppes on the western QTP under a cold and moist climate.

In summary, the plateau climate was becoming wetter and warmer, forming wetlands in the basins and valleys resulting in blanket bogs consisting of peat and thick layers of humus. The thick-lyered peat at the bottom of soil profiles in Wumaqű, Damxung and Qinongga, Yangbajing, in the Tibet Autonomous Region were AMS-^{14}C-dated at 8175±200−9970±135 a BP, indicating the start of peat formation (Li, 1982). Dark silty sand clay is found at depths of 2.5−3.0 m in the Borehole CK80 at Qingshui'he Riverside along the QTH. There a soil sample at depths of 2.7−3.0 m was dated at 8800±305 a BP. Meanwhile, the lithology change upwards from yellow sand clay and medium-fine sand with limestone blocks and carbonate nodules at the bottom to dark silty sand clay deposits at the upper part. This transition is a result of climate warming and wetting and subsequent enrichment of organic matter. In addition, humic silt and sand at the upper part of sand wedges on the second terrace of the Zuomoxikong Qű (River) in the Fenghuoshan Mountains along the QTH is dated at 9218±189 a BP, while that at the Highway Maintenance Squad Station (HMSS) 82 along the QTH at the southern piedmont of the Fenghuoshan Mountains was dated at 9160±170 a BP. They all indicate an ameliorating climate and no growth of frost cracks and cryogenic wedges. This warming climate was conducive to plant growth, and as a result, some sand dunes formed during the end of the Late Pleistocene were largely stabilized. Thus, buried plant roots and stems in the sand ridges 2 km southeast of Wudaoliang along the QTH have been ^{14}C-dated at 9716±270 a BP (Wang, 1989).

4.3 Local Holocene Megathermal Period (LHMP) (8500−7000 to 4000−3000 a BP: intensive permafrost degradation

The mid-Holocene is the optimal climate period in the Holocene, so it is also called the hypsithermal period, or LHMP. According to Shi et al. (1992), the LHMP in China occurred during 8500−3000 a BP, with a stable warm and wet climax at 7200−6000 a. During the LHMP, it was 1−2°C warmer than today in South China and in the middle- and down-

streams of the Yangtze River Basin, 3°C warmer than today in North, Northeast and West China, 4−5°C warmer than today on the QTP in Southwest China, and the warming in winter was much more pronounced. For example, in the ice-core record from Gulia Ice Cap, at the climax of the LHMP, δ^{18}O was 3‰ higher than the average of the δ^{18}O during the last millenium, i.e., a warming of about 4−5°C (Shi, 2006). The climate warming in the arid regions in North China could have been about 1.0−3.5°C in MAAT (with an uncertainty of 20−130%); annual precipitation increased by 30−400 mm (with an uncertainty of 10−120%). The increase in annual precipitation also had a trend of inland increasing from Southeast China to Northwest China (Yu et al., 2013).

The field surveys indicate that the ice wedges in Wuma in northern part of the Da Xing'anling Mountains were formed during the LLGM and were preserved well before the last inspection in 2007. There were thawed concavites on the top 0.7 m of the ice wedges, an evidence for the lowering permafrost table. This implies that in spite of a warming climate during the LHMP, the periglacial environment still prevailed in the area (Tong, 1993; Jin et al., 2016). In addition, in the Amu'er in northern part of the Da Xing'anling Mountains (52°51′N, 123°11′E), analysis on the light and heavy mineral contents of Quaternary deposits indicate low contents of unstable and relatively stable minerals, and even less stable minerals (<5%); in contrast to 75−92% in the gravels (Guo et al., 1981). This also indirectly demonstrates that the northern part of the Da Xing'anling Mountains have never undergone a long-term warm and wet climate. The above-mentioned two areas are now still in the continuous permafrost zone.

With rising temperature in the LHMP, permafrost in China retreated extensively, and latitudinal permafrost disappeared from eastern Inner Mongolia, eastern Xinjinang, and North China. Most latitudinal permafrost in Northeast China also disappeared, or retreated to the northwestern corner (north of Amu'er-Mangui) of the Da Xing'anling Mountains to the north of 51°−52°N (Figure 3). Because of the northward retreat of the SLP by 3°−4°N, the climate warming could be about 3−4°C warmer than today.

The age data on the formation of thick peat and humus layer on the QTP, as listed in the Appendix 1, are largely grouped in the LHMP, indicating a warm and wet climate. Along the QTH, the ^{14}C-age of the humus soil at the depth of 4.4 m in the Borehole No. 8 at Xidatan is 7530±300 a BP, and that of ash-like humic sand on the first terrace of Nachitai is 4910±100 a BP; anthropic fire-used ash sites have been found in many places from Nachitai to Xidatan along the Kunlun River, indicating a suitable climate and environment for human activites; the age of humus layer at the HMSS 109 on the southern slopes of Tanggula Mountains is 5058±443 a BP, and that at HMSS 120 is 4313−4576 a BP. The completion time for the continuous deposition of thick peat was 3050±120 a BP at Qinongga, Yangbajiang, Tibet Autonomous Region and 3575±80 a BP at Wuma Qű (River), Damxun, Tibet Autonomous Region.

On the northeastern and eastern QTP, the middle part of a 2-m-thick humus soil profile on the eastern slope of Mount Ri'yueshan is dated at 4920±80 a BP while the peat at the depth of 2 m in a 5-m-thick peat soil profile on southern slope of Heka South Mountains is dated at 4625±117 a BP. A thick humus soil is dated at 4395±215 a BP at a gelifluction tongue in the Wenbo South Mountains in Shiqu, Sichuan Province, while the peat is dated at 5422±94 a BP in the lower part of a 4.15-m-thick peat deposit on the morainic platform in the Nianbao'yeze Mountains. A layer of 5.2 m of peat was deposited during 9350−370 a BP in the Peat Farm soil profile in the outskirts of Hongyuan, Zoîgé Plateau, Sichuan Province, and a layer of 3.3 m peat was formed during 6350−3250 a BP (Sun, 1998).

The above-mentioned extensive and thick deposits are all products in the LHMP as long as 4000−5000 years. They appear to be an indirect indictor of large-scale and intensive degradation of permafrost. In the later LHMP (ca. 4000−3000 a BP), the LLP was 300−500 m higher than today; to the north of Kunlun Mountains and to the south of Tanggula Mountains, permafrost had been converted into seasonally frozen ground. In the Chumar'he High Plain between the Kunlun and Tanggula mountains, permafrost was thawing continuously for a long time, reaching to a depth of 14−16 m (Jin et al., 2007a) and resulting in a vertical detachment of permafrost from the active layer (Jin et al., 2006). In the meantime, a thick-layered ground ice was formed at depths of 14−16 m, i.e., the position of paleo-permafrost table (Xin and Ou, 1983). Due to the thawing of shallow permafrost and ground ice, numerous thermokarst lakes and depressions were formed, and ice wedge pseudomorphs were formed after ice melting, on the QTP.

During the LHMP, permafrost on the plateau was sporadic and isolated, or deeply buried (Jin et al., 2009). However, at high elevations, such as in the Kunlun, Fenghuoshan and Tanggula mountains, it was still dominated by continuous permafrost. In the meantime, permafrost degraded more intensely on eastern QTP as represented by that along the Qinghai-Kang (W Sichuan) Highway (QKH) than that in the interior QTP as represented by that along the QTH and western QTP. Along the QKH, permafrost was completely converted to seasonally frozen ground at elevations below 4200 m asl; while at 4200−4400 m asl (Hua'shixia to Qingshui'he), the permafrost thawed down to depths of 15−25 m, with a 3-dimensional thawing (vertical and lateral) (Jin et al., 2006, 2009; Chang et al., 2017). In the end, deeply buried permafrost was left at depths of 10−20 m in some well-preserved areas in the Bayan Har and Anemaqên mountains along the QKH, and in the Source Area of the Yellow River (Jin et al., 2006a, 2009). In some areas further to the east, permafrost was thawed completely at lower

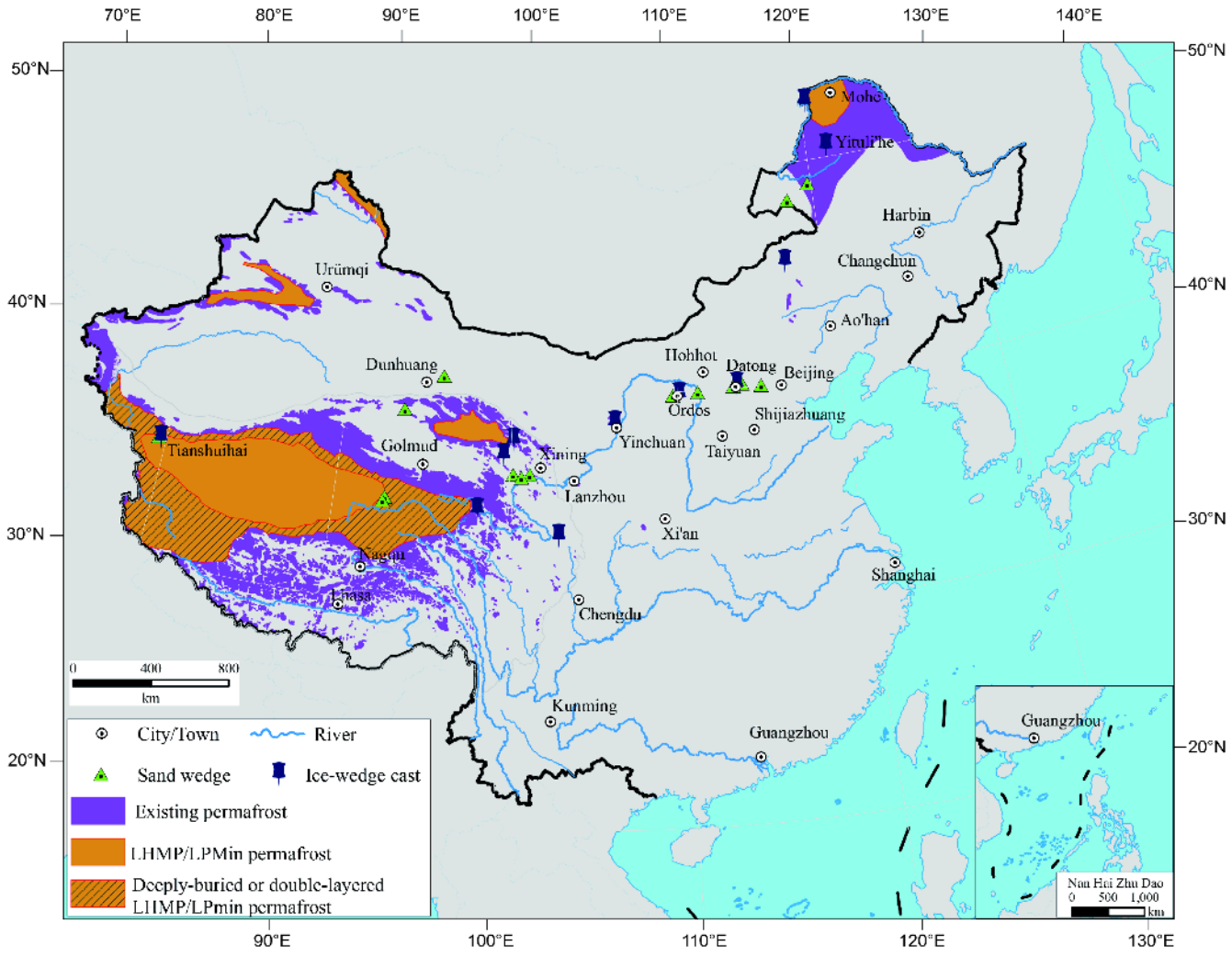

Figure 3 Distribution of permafrost in China during the LLPMin/LHMP, and at present.

elevations, leaving behind only some isolated permafrost islands on the top of Bayan Har and Anemaqen mountains.

If calculated by an elevation of the LLP by 300−500 m, permafrost could only be preserved on the top or upper parts of these high mountains in western China, such as in the Tianshan, Altai and Qilian mountains. The Tarim, Turpan and Zhunger bains are at 41°−46°N, similar to that of Songhuajiang-Liao'he Basin in Northeast China. Thus, permafrost should have vanished in the major basins during the LHMP. Calculations based on Figure 2 indicate only an areal extent of 800000−850000 km^2 for the remained permafrost in China during the late LHMP, or about 50% of existing permafrost extent at present.

During the late LHMP, westward shifts of vegetation zones occurred under a warming and wetting climate; it was acompanied also by vertical and horizontal shifts as well. In the peripheries of high mountains and plateaux, timberline became lower, while in West China, steppes expanded and deserts shrank. The transition zone (meadow steppes) between forest and steppe belts evidently moved westwards to northeast of Manzhouli-Buhat Banner-Hoh Hot-Helanshan South-Xi'ning, a westward movement of 3°−5°E in comparison with today. In the meantime, the boundary between temperate forest-steppe and typical steppe also shifted westward by 3°−4°E. Forest-steppe environment dominated the Altai and Tianshan mountains, while plateau steppe and forest dominated the QTP. The areal extent of semi-deserts and deserts dramatically shrank, with only some patches remaining in the middle Tarim Basin, middle and western Inner Mongolia Plateau and Chaidam Basin. Vegetation zones on southern and eastern QTP, such as in the Hengduan Mountains, also shifted to varied extents (Tang and Shen, 1996).

4.4 Neoglaciation in the late Holocene (4000−3000 to 1000 a BP): second major permafrost expansion

In the late Holocene (4000−3000 a BP), the climate started cooling again. The ice-core record from the Dunde Glacier in the Qilian Mountains indicates a cooling that started ca. 4 ka

BP, and reached the coldest period during 2800−2700 a BP. Hence, the cooling fluctuated until 1000 a BP. This is the so-called Neoglaciation period in the late Holocene. With the uplifting of the QTP, the climate kept cooling, and mountain glaciers advanced extensively. Three to four terminal and lateral morains were left behind in the Kunlun and Tanggula mountains, such as the Neoglacial lateral moraines dated at 3983−3522 a BP in the Congce Ice Cap in the Kunlun Mountains (Zheng, 1990).

A string of pingos were formed at 4250−4300 m asl along the fault in eastern Xidatan along the QTH; intensive cryoturbations were developed at about 3800 m asl on the first terrace of the Kunlun River south of Nachitai along the QTH. The thick layer of humus formed during the LHMP near the HMSSs 100 and 120 on southern slopes of Tanggula Mountains were re-frozen. Pingo groups 40 km east of Shiqu County Town, Sichuan Province on eastern QTP were formed at 2925±175 a BP; those at the northern side of K65 along the Maqên-Changma'he Highway were formed at 3925±185 a BP. Large polygons, gelifluction landforms and stone circles, and other periglacial phenomena were extensively developed during the Neoglaciation period, such those on the Mt. Ri'yueshan (>3450 m asl), Öla Mountain Pass (>3750 m asl) along the QKH and northern slopes of the Bayan Har Mountains (4000−4100 m asl). All these paleo-permafrost and periglacial remains prove a relatively cold climate, when a 20-m-thick permafrost was developed near the Borehole No. 8 in Xidatan along the QTH.

By comparing spatiotemporal variations in these periglacial remains, it can be deduced that the LLP was then 300 m lower than that of preesent, and the MAAT, about 2°C lower than today. On the basis of intensive degradation of permafrost during the LHMP, permafrost reappeared, and expanded radially from the interior QTP, and reached the maximum permafrost extent in the Neoglacial period by 1000 a BP, which was about 20−30% larger than today. In the Neoglacial period, along the QTH the northern LLP was at 3700−3800 m asl south of Nachitai, and the southern LLP was at 4400−4500 m asl in the Damxung Valley. On the Chmar'he High Plain between the Kunlun and Tanggula mountains (>4500 m asl), permafrost refroze downwards, forming a layer of epigenetic permafrost 30 m in thickness (Ding and Guo, 1982). This layer was detached from the residual permafrost of the LHMP. Therefore, so far there has been no buried or double-decked permafrost found on the Chumar'he High Plain along the QTH.

This contrasts with many places on northeastern QTP, such as Hua'shixia to Qingshui'he along the QKH, and to the east where buried permafrost and thawed nuclei (talik) have been discovered. This might be attributed to the fact that these areas are on the eastern margins of the plateau permafrost zone, and downward thawing during the LHMP reached depths of 15−25 m, but the epigenetic permafrost of Neoglaciation was thinner than 15−25 m, resulting in vertical detachment of permafrost and resultant buried and/or double-decked permafrost layers. It is also possible that in some areas, due to secondary (second-tier) climate warming, the Neoglacial permafrost was thawed to certain depths, resulting a mosaicked distributive features of interwoven multi-layered permafrost and taliks (Jin et al., 2006a, 2007a, 2009; Chang et al., 2017). Cold air drainage could possibly be involved.

On the first terrace south of Yituli'he (50°32′N, 129°29′E) in the northern Da Xing'anling Mountains, Neoglacial ice wedges have been discovered and ^{14}C-dated at 3600–1600 a BP, indicating three cooling periods of 2800 a BP (2.1°C), 2300 a BP (1.1°C) and 1900 a BP (1.3°C) (Yang and Jin, 2010; Yang et al., 2015). It thus concluded that there was a cooling of about 2°C, and a southward shift of the SLP by about 2°N.

4.5 Medieval Warming Period (MWP) (1000 to 500 a BP): relative permafrost degradation

After the Neoglaciation, China experienced serveral small-scale climate fluctuations, among which the Sui and Tang dynasties (AD 581−907) were in warm periods. The warming started in Shang Dynasty (ca. 1600−1046 BC), reached maxima in Zhou (ca. 1046−221 BC), Han (202 BC to AD 220) and until Tang dynasty (AD 618–907), with a warming of about 1.5°C for centuries, but there were also cooling in the Sui Dynasty (AD 581−618), but the cooling was mainly limited to the South and North States (AD 420−589) and was cooler than today (Zhu, 1972). Because of the short history to date, most paleo-periglacial landforms of this period were well preserved and the remains of paleo-permafrost were distinct on the QTP.

The pingos formed in Xidatan, K40 East of Shiqu, West Sichuan Province and K65 along the Maqên-Changma'he Highway during the Neoglaciation were thawed, forming pingo scars. The humus soils in the center of the thawed depressions were dated at about 720−625 a BP, after the permafrost had been thawed at these locations.

This was a period for regional permafrost degradation on the QTP. Downward thawing of permafrost reached the depth of about 10 m at lower elevations. For example, the lower layer of permafrost, as revealed at depths of 9.7−12.3 m in Borehole CK1 in Dinaran northeast of Hua-shixia and at depths of 11.6−15.2 m in Borehole ZK8 in Changma'he, was the residual permafrost during the MWP (Jin et al., 2006a, 2007a).

Accordingly, the upper layer of permafrost as found at depths of 7.5−9.0 m on the Chumar'he High Plain, and in the Fenghuoshan Mountains in particular along the QTH, was formed during the MWP. For example, there were two positions of paleo-permafrost tables in the Borehole CK224 on

the Chumar'he High Plain, the upper one of the MWP at 8.4 m in depth, and the lower one of the LHMP at 16 m. Thick-layered ground ice were encountered under these permafrost tables (Xin and Ou, 1983). The degradation of permafrost during the MWP resulted in a higher LLP of about 150−250 m above the present LLP, while the SLP moved northwards by 1°−2°N. As a result, the permafrost extent in China during the MWP was about 20% less than today.

4.6 Little Ice Age (LIA, 500 to 100 a BP) in the late Holocene: Relative permafrost expansion

The Little Ice Age (LIA) is the cold period in the 15th−19th century, with the latest permafrost expansions and glacier advances, which was recorded in ice-cores and glacial deposits. In the ice-cores from the Dunde Glacier No. 1 in the Qilian Mountains, the three coolings occurred in AD 1420−1520, 1570−1680, and 1770−1890. The second cold period (16th and 17th centuries) was the coldest among the three, with a cooling of about 1.5°C colder than today.

It was a time when the QTP was drying and cooling, which was accompanied by permafrost expansion and thickening, and new permafrost islands were formed in the peripheries of the QTP. Along the QTH, a permafrost layer was formed by the downward freezing, which was re-attached with the upper paleo-permafrost (table) formed during the MWP in the late Holocene. For example, the humus layer at the HMSS 121 along the QTH formed since the last 780 a BP was refrozen. On eastern QTP, the thin permafrost of the LIA was unable to attach to the underlying permafrost layer, such as the permafrost layer found at depths of 1.5−8.0 m in Borehole ZK6 on the northern bank of the Ngöring Lake and at depths of 5.3−8.2 m in the water well in the Qingshui'he Town on the southern slope of the Bayan Har Mountains along the QKH (Jin et al., 2006a, 2006b)

Active rock glaciers, block fields, stone stripes, or other similar sorted patterned ground or ice-contained permafrost can indicate the occurrence of permafrost (Tian, 1981; Gao, 1983). Barsch (1978) first pointed out that rock glaciers could indicate the LLP of discontinuous alpine permafrost. Therefore, Jakob (1992) estimated the LLP of discontinuous alpine permafrost at about 5560−5360 m asl (sunny slopes) and 4959−5050 m asl (shadowy slopes) in the Kunbu Himalayas, Nepal on the basis of active rock glaciers and seismic geophysical data in the vicinity of Poklade Cliff (27°55′N, 86°50′E), whereas the lower limit of active rock glaciers there is at about 5000−5300 m asl. These results agree well with the calculated result from the Gauss curve for the location (⩾ 5080 m asl, 25°22′N) (Cheng and Wang, 1982). On the basis of the distribution of protalus and morainic rock glaciers, Owen and England (1998) deduced that the LLP of discontinuous permafrost should be higher than 4000 m asl in western Himalayas and Karakurums in northern Pakistan and India. Similarly, it can be deduced that during the LIA, (inactive) stone fields and (inactive) stone stripes were above 4130 m asl along the road side of Rizha Village, Darag County, Qinghai Province. At the lower limit of these stone fields and stripes, the underlying humic soils are dated at 422±85 a BP, which should be older than the overlying stone streams or stripes. Therefore, those inactive stone fields and stone stripes/streams were formed during the LIA. At present, the LLP at this location is at 4300 m asl. Thus, the LIA had a cooling of about 1.0−1.5°C, a lowering of LLP by 150−200 m, and with a permafrost extent of 1.5×10^6 km^2, or about 15−20% greater than today.

During the LIA, plateau lakes shrank continuously, and some small and medium lakes dried up. Most of the lakes became saline and salt lakes, such as the salt lake behind the HMSS 69 along the QTH, where silty soil under a 60-cm-thick salt crust was dated at 1094±433 a BP; the silt under a 50-cm-thick salt layer in the Hajiang Salt Lake to the east of Ngöring Lake was dated at 1080±260 a BP. In the meantime, those (semi)fixed sand dunes were re-activated on the surface, and covered by aeolian sand, result in worsening land desertification.

4.7 Recent warming (since 100 a BP, i.e., the 20th century): persistent permafrost degradation

During the last century, especially the last few decades, the effect of greenhouse gases may have caused and sustained climate warming. Large amounts of data indicate a global warming of about 0.3−0.8°C since AD1880; in particular, the climate since the 1980s has been the warmest since the meteorological record started. During the last four decades, the MAAT in the permafrost regions on the QTP has risen by 1.12°C, at a warming rate of 0.025−0.030°C yr^{-1}, much greater than that of the periphery non-permafrost regions (0.017−0.019°C yr^{-1}) (Jin et al., 2011a). Particularly, since the 21st century, the climate warming has been accelerated, and mean annual ground surface temperature has risen by 1.34°C. The climate in Northeast China has warmed by 1.7°C during the last 100 years, the Da Xing'anling Mountains having experienced the most pronounced warming. The last three decades in the 20th century have witnessed a rise in MAAT by 1.4−2.0°C. It is evident that during the last six decades, there have a clear patten in changes in ground surface temperatures. There was a cold period during the 1950s to 1970s, followed by a warming since the 1980s; the coldest occurred in the 1950s, with a departure of −0.8°C; the warmest occurred in the 2000s, with a departure of +1.1°C. However, the climate warming again was the most pronounced in the Da Xing'anling Mountains, with a warming rate of 0.038−0.040°C/a in the MAAT during the last 30 years (Luo et al., 2014). Climate warming has resulted in

Table 1 Summary of changes in permafrost in China during the last 20 ka

Climate period	Absolute age	Changes in permafrost features	Climate & cooling (°C)	Change in		Permafrost extent (10^6 km^2)	Percentof today (%)	Major direct evidence	Major indirect evidence	Major references
				SLP (°N)	LLP (m)					
Local Last Glacial Max (LLGM) in Late Pleistocene	ca. 20 to 13–10.8 ka BP	Ice-wedges developed over the entire permafrost area	Cold/moist (dry), 4–5 (NE China), 3–11 (N China, 7–9 (QTP)	S ↓4–5 (NE China)	↓1200–1400	5.3–5.4	>300	Cryogenic wedges of all types	Glacial land-forms, ice cores, ice-wedges, paleo-timberline, pollen, sandland, cold climate fauna & flora, models	Zhang, 1983; Xu and Pan, 1990; Wang and Bian, 1993; Tong, 1993; Pan and Chen, 1997; Cui et al., 2004; Cheng et al., 2006; Jin et al., 2006a, 2007a, 2016; Chang et al., 2011, 2017; Zhao et al., 2013
Dramatic climate changes in early Holocene	10.8 to 8.5 −7 ka BP	Relative stable & degrading permafrost	Drying/cooling, then warming/ wetting, very unstable	Retreat, started to disappear on Sanjiang Plain	600–700	2.2–2.4	140–150	Pingo scars, sand wedges	Ice core, diatom, pollen, peat, sand dunes, …	Li, 1982; Wang, 1989; Li and Jiao, 1990; Song and Xia, 1990; Yao and Shi, 1992; Tang and Shen, 1996
Mid-Holocene Megathrmal Period (LHMP)	8.5–7 to 4 −3 ka BP	Intensive degradation	Wet/warm, 2–3 (most parts), 4–5 (QTP), 1.0–3.5 (N China)	N 3–4 (NE China)	300–500 (QTP, mountains in W China)	0.8–0.85	50	Ice wedges, buried permafrost, ground ice, thermokarst lakes, paleopf gelifluctions, pingo scars	Mineral analysis, peat, ice-core (δ^{18}O), sand dunes, human fire use, timberline, pollens	Guo et al., 1981; Xing and Ou, 1983; Tong, 1993; Tang and Shen, 1996; Sun, 1998; Jin et al., 2006a, 2007a, 2009, 2016; Shi, 2006; Yu et al., 2013
Late Holocene cold period (Neoglaciation)	4–3 to 1 ka BP	2nd expansion	Fluctuatingly cooling −2 to −1 (NE China, QTP)	S ↓ 2 (NE China)	↓ ca. 300 (QTP)	1.9–2.1	120–130	Pingo scars, cryoturbations, polygons, gelifluctions, ice wedges	Ice core, glacial till, peat, detached or buried permafrost	Ding and Guo, 1982; Zheng, 1990; Jin et al., 2007a, 2009, 2011b, 2016; Yang and Jin, 2010; Yang et al., 2015; Chang et al., 2017
Late Holocene warm period (MWP)	1–0.5 ka BP	Relative retreat	Wet/warm, 1.5	N 1–2	ca. 150–250	1.4–1.5	80	Pingo scars, buried permafrost, ground ice	Phenology, humus	Zhu, 1972; Xing and Ou, 1983; Jin et al., 2006a, 2007a
Little Ice Age (LIA)	500–100 a BP	Relative expansion	Fluctuatingly cooling −1.5 to −1	S ↓ 1–1.5	↓ ca. 150 −200	2.1–2.2	115–120	Paleopf, detached permafrost, stone fields & streams	Ice-core, till, humus, silt in salt lake, sand land	Jin et al., 2006a
Recent warming	100–0 a BP	Persistent degradation	Warm/dry 0.3–0.8	N 0.5–1.5	50–100	1.59	100	Ground temp, LLP/SLP, areal extent survey abd measurement	Measurement and thermokarsts	Jin et al., 2006a, 2011b, 2016; Ran et al., 2012

persistent permafrost degradation, and particularly since the 21st century, permafrost degradation has been accelerating. The areal extent of permafrost in China has been reduced to 1.59×10^6 km^2 from 1.59×10^6 km^2 (Zhou et al., 2000; Ran et al., 2012) .

4.8 Changes of permafrost in China during the last 20 ka: patterns, processes and trends

In summary, since the LLGM although there have been occasional permafrost expansions in cold periods, such as the Neoglaciations and LIA, the areal extent of permafrost in China in general has been on the decline under a fluctuatively warming climate (Table 1). The areal extent of permafrost during the LLGM was close to its maximum at 20 ka BP and the LHMP could have reached its minimum despite the substantial expansions during the Neoglaciations and LIA. During the MWP and since the last century, China has witnessed the most intensive, rapid and extensive permafrost degradation since the LHMP, and this trend is currently being enhanced. Because of these changes, the areal extent of permafrost in China has shrunk from 5.30×10^6–5.40×10^6 km^2 at the LLGM/LLPMax to 0.80×10^6–0.85×10^6 km^2 at the LHMP/LLPMin, and then back to the present 1.59×10^6 km^2.

5. Conclusions and prospects

Since the last 20 ka, China has experienced many major climatic, environmental and geocryological changes, such as the LLGM/LLPMax at the end of the Late Pleistocene and the LHMP/LLPMin in mid-Holocene. On the basis of paleo-permafrost and periglacial remains, in combination with glacial, palentological and other records, it is estimated that during the LLGM, in comparison with today, the MAAT was about 7−9°C colder on the QTP, 4−5°C colder in the Da and Xiao Xing'anling Mountains, and 5−12°C colder in arid regions in North China; during the LHMP/LLPMin, in comparison with today, the MAAT was about 4−5°C warmer than today on the QTP, 3−4°C warmer in the Xing'anling Mountains, and 1−3.5°C colder in arid regions in North China. Accordingly, permafrost has changed substantially. The latest data indicate a present extent of permafrost in China at 1.59×10^6 km^2, shrinking from 5.3×10^6–5.4×10^6 km^2 during the LLGM/LLPMax, or three times of today. However, during the LHMP/LLPMin, that was reduced to 0.80×10^6 −0.85×10^6 km^2, or about 50% of the current permafrost area. That in other periods falls in between the LLPMax and LLPMin.

According to the ages and distributive features of paleo-permafrost in China, after the delineation of permafrost patterns in the LLPMax/LLPMin, the evolutionary processes of permafrost in China can be divided into seven periods: (1) LLGM/LLPMax in the Late Pleistocene ca. 20 to 13−10.8 ka BP); (2) dramatic changes in climate and permafrost in early Holocene (10.8 to 8.5−7 ka BP); (3) Local Mid-Holocene Megathermal Period (LHMP, 8.5−7 to 4−3 ka BP); (4) Late Holocene cold period, or Neoglaciation (4−3 to 1 ka BP); (5) Late Holocene warm period (Medieval Warm Period, MWP, 1000−500 a BP); (6) Late Holocene cold period (Little Ice Age, LIA, 500−100 a BP), and (7) recent warming period (100−0 a BP, 20th century upto date). Paleo-climate, -geography and -environment, and permafrost features were reconstructed for the seven periods.

The formation, development and changes of permafrost in China are complicated due to the combined influences from climate changes of varied spatiotemporal scales and human activities and subsequent interwoven impacts. They have resulted in concurrent processes of permafrost formation and development as well as degradation at the same time in different regions and at different depths. This is particularly true for shallow permafrost and the permafrost layer in the peripheries of permafrost zones where climatic fluctuations of different amplitudes and intensity have induced repreated freezing and thawing, forming mosaicked distributive patterns of permafrost and talik. As a result, the dating of permafrost remains a major challenge in Quaternary geocryology in China. In particular, rapid, large-scale and intensive economic development have tremendous adverse impacts on Quaternary permafrost and periglacial landforms, it deems necessary to timely rescue and study these precious evidence and records.

Permafrost should have developed in Tarim and Zhunger basins in Xinjiang, West China during the LLGM/LLPMax taking into account of their latitudes and elevations. However, so far no reliable paleo-permafrost and -periglacial evidence has been discovered in the interiors of the two basins. Was there permafrost in their history? This is also true for other sand lands and deserts/gobi in North China and adjacent regions or countries. The relationships between permafrost and deserts in China and bordering regions await for reliable data and further investigations.

Acknowledgements *We greatly appreciate the support of Professor Hua'yu Lu at the Nanjing University in timely providing the OSL dating; remarks and advice from Academician Zhengtang Guo and other colleagues in the Strategic Pilot Science and Technology Program of the Chinese Academy of Sciences (Grant No. XDA05000000, Identification of carbon budgets for adaptation to changing climate and the associated issues). Authors also would like to thank two unidentified reviewers for their constructive review opinions. This work was supported by the National Natural Science Foundation of China and Russian Foundation for Basic Research (FRBR) on "Formation, evolution and changes of Pleistocene cryogenic deposits in Eastern Asia" (Grant No. 41811530093), the Key Program of the Department of International Cooperation of the Chinese Academy of Sciences (Assessment of changes in permafrost in China, Russia and Mongolia and their impacts on key engineering infrastructures), (Permafrost extent in*

China during the Last Glaciation Maximum and Megathermal) of the Strategic Pilot Science and Technology Program of the Chinese Academy of Sciences (Grant No. XDA05120302), and the CAS Overseas Professorship of Sergey S. Marchenko, and under the auspices of the International Permafrost Association Working Group on Global Permafrost Extent During the Last Permafrost Maximum (LPM).

References

Barsch D. 1978. Rock glaciers as indicators of discontinuous alpine permafrost: An example from the Swiss Alps. In: Proceedings 3rd International Conference on Permafrost. Washington D C: National Academy Press. 136−141

Böhner J, Lehmkuhl F. 2005. Environmental change modelling for Central and High Asia: Pleistocene, present and future scenarios. Boreas, 34: 220–231

Chang X, Jin H, He R. 2011. Formation and environmental evolution of sand wedges on the Tianshuihai North lakeshore in the western Kunlun Mountains (in Chinese). Quat Sci, 31: 112−119

Chang X L, Jin H J, Zhang Y L, He R X, Luo D L, Wang Y P, Lü L Z. 2015. Thermal impacts of boreal forest vegetation on active layer and permafrost soils in northern da Xing'Anling (Hinggan) Mountains, Northeast China. Arct Antarct Alp Res, 47: 267–279

Chang X L, Jin H L, Wang S L. 2017. Evolution of permafrost on the Qinghai-Tibet Plateau and its impacts on aeolian environments. Sci Cold Arid Reg, 9: 1−19

Cheng G, Wang S. 1982. On the zonation of high-altitude permafrost in China (in Chinese). J Glaciol Cryopedol (Geocryol), 4: 1−17

Cheng J, Zhang X, Tian M, Yu W, Tang D, Yue J. 2006. Ice wedge casts discovered in the source area of Yellow River, northeast Tibetan Plateau and their paleoclimatic implications (in Chinese). Quat Sci, 26: 92−98

Cui Z. 1980. Periglacial phenomena on the Qinghai-Tibet Plateau and their environmental significance. In: Collection Papers for International Communications on Geology (5) (in Chinese). Beijing: Geology Press. 109−122

Cui Z, Zhao L, Vandenberghe J, Zhang W. 2002. Discovery of ice wedge and sand-wedge networks in Inner Mongolia and Shanxi Province and their environmental significance (in Chinese). J Glaciol Geocryol, 24: 708−717

Cui Z, Yang J L, Zhao L, Zhang W, Xie Y Y. 2004. Discovery of a large area of ice-wedge networks in Ordos: Implications for the southern boundary of permafrost in the north of China as well as for the environment in the latest 20 ka BP. Chin Sci Bull, 49: 1177

Ding D, Guo D. 1982. Preliminary discussions on the evolutionary history of permafrost on the Qinghai-Tibet Plateau. In: Geographical Society of China, ed. Proceedings of Chinese Conference on Glaciology and Geocryology (Geocryology Volume) (in Chinese). Beijing: Science Press. 78−82

Du N, Kong Z, Shan F. 1989. A preliminary investigation on the vegetational and climatic changes since 11000 yearsin Qinghai Lake-An analysis based on palynology in core QH85-^{14}C (in Chinese). Acta Bot Sin-J Integrat Plant Biol, 30: 803−814+825−826

French H M. 2018. The Periglaical Environment. 4th Ed. Hoboken: John Wiley & Sons. 1−515

Gao F. 1983. Ancient rock sea in Shennongjia Mountain (in Chinese). J Glaciol Cryopedol (Geocryol), 5: 67−69

Guo D, and Li Z. 1981. Preliminary approach to the hisory and age of permafrost in Northeast China (in Chinese). J Glaciol Cryopedol (Geocryol), 3: 1−14

Guo D, Wang S, Lu G, Dai J, Li E. 1981. Division of permafrost regions in Daxiao Hinggan Ling, Northeast China (in Chinese). J Glacilo Cryopedol (Geocryol), 3: 1−9

Harris S A, Jin H J. 2012. Tessellons and sand wedges on the Qinghai-Tibet Plateau and their palaeo-environmental implications. In: Proceedings 10th International Conference on Permafrost. Salehard. 149–154

Harris S A, Jin H J, He R X. 2016. Very large cryoturbation structures of Last Permafrost Maximum age at the foot of Qilian Mountains (NE Tibet Plateau, China): A discussion. Permafrost Periglacial Process, 28: 757–762

Harris S A, Bruchkov A, Cheng G. 2017. Geocryology—Characteristics and Use of frozen Ground and Permafrost Landforms. Boca Raton (FL): CRC Press.1−765

Harris S A, Jin H, He R. 2018. Tessellons, topography, and glaciations on the Qinghai-Tibet Plateau. Sci Cold Arid Reg, 10: 187–206

Heyman J. 2010. Paleoglaciology of the northeastern Tibetan Plateau. Doctoral Dissertation. Stockholm: Stockholm University. 11

Heyman J, Hättestrand C, Stroeven A P. 2008. Glacial geomorphology of the Bayan Har sector of the NE Tibetan Plateau. J Maps, 4: 42–62

Heyman J, Stroeven A P, Alexanderson H, Hättestrand C, Habor J, Li Y K, Caffee M W, Zhou L P, Veres D, Liu F, Machiedo M. 2009. Palaeoglaciation of Bayan Har Shan, northeastern Tibetan Plateau: Glacial geology indicates maximum extents limited to ice cap and ice field scales. J Quat Sci, 24: 710–727

Jakob M. 1992. Active rock glaciers and the lower limit of discontinuous alpine permafrost, Khumbu Himalaya, Nepal. Permafrost Periglacial Process, 3: 253–256

Jiao S, Wang L, Sun C, Yi C, Cui Z, Liu G. 2015. Discussion about the variation of permafrost boundary in Last Glacial Maximum and Holocene Megathermal, Tibetan Plateau (in Chinese). Quat Sci, 35: 1−11

Jiao S, Wang L, Liu G. 2016. Prediction of Tibetan Plateau permafrost distribution in global warming (in Chinese). Acta Sci Nat Universit Pekinen, 52: 249−256

Jin H, Zhao L, Wang S, Guo D. 2006a. Evolution of permafrost and environmental changes of cold regions in eastern and interior Qinghai-Tibetan Plateau since the Holocene (in Chinese). Quat Sci, 26: 198−210

Jin H, Zhao L, Wang S, Jin R. 2006b. Thermal regimes and degradation modes of permafrost along the Qinghai-Tibet Highway. Sci China Ser D-Earth Sci, 49: 1170–1183

Jin H J, Chang X L, Wang S L. 2007a. Evolution of permafrost on the Qinghai-Xizang (Tibet) Plateau since the end of the late Pleistocene. J Geophys Res, 112: F02S09

Jin H J, Yu Q H, Lü L Z, Guo D X, Li Y W. 2007b. Degradation of permafrost in the Xing'anling Mountains, northeastern China. Permafrost Periglacial Process, 18: 245–258

Jin H J, He R X, Cheng G D, Wu Q B, Wang S L, Lü L Z, Chang X L. 2009. Change in frozen ground and eco-environmental impacts in the Sources Area of the Yellow River (SAYR) on the northeastern Qinghai-Tibet Plateau, China. Environ Res Lett, 4: 045206

Jin H J, Luo D L, Wang S L, Lü L Z, Wu J C. 2011a. Spatiotemporal variability of permafrost degradation on the Qinghai-Tibet Plateau. Sci Cold Arid Reg, 3: 281−305

Jin H, Chang X, Guo D, Yang S, He R. 2011b. Holocene sand soil wedges on the south-central Hunlun Buir High Plain in Northeast China (in Chinese). Quat Sci, 31: 765−779

Jin H J, Chang X L, He R X, Guo D X. 2016. Evolution of permafrost and periglacial environments in Northeast China since the Last Glaciation Maximum. Sci Cold Arid Reg, 8: 269−296

Ju L X, Wang H K, Jiang D B. 2007. Simulation of the last glacial maximum climate over East Asia with a regional climate model nested in a general circulation model. Palaeogeogr Palaeoclimatol Palaeoecol, 248: 376–390

Li B Y, Li J J, Cui Z J, Zheng B X, Zhang Q S, Wang F B, Zhou S Z, Shi Z H, Jiao K Q, Kang J C. 1991. Quaternary Glacial Distribution Map of Qinghai-Xizang (Tibet) Plateau. Beijing: Science Press

Li F. 1990. Features of paleo-periglacial strucutures on the Sanjiang Plain, Northeast China and their environmental implications. In: Formation and Evolution of Quaternary Natural Environment on NE China Plain, China (in Chinese). Harbin: Harbin Cartography Press. 202−208

Li S, Jiao K. 1990. Glacier variations on the south slope of West Kunlun Mountains since 30000 years (in Chinese). J Glaciol Geocryol, 12: 311−318

Li S, He Y. 1990. Basic features of permafrost in the West Kunlun

Mountains. In: Lanzhou Institute of Glaciology and Geocryology, Chinese Academy of Sciences, ed. Collection Papers 4th Chinese Conference on Glaciology and Geocryology (Geocryology Volume). Beijing: Science Press. 1−8
Li X. 1982. ^{14}C dating of humus layer in the Damxung and Yangbajing basins, Xizang (Tibet) Autonomous Region, China and its significance. In: Editorial Committee of the Collection Papers for the Geology of Qinghai-Xizang (Tibet) Plateau, Ministry of Geology and Minerals, PRC, ed. Collection Papers for Geology of Qinghai-Xizang (Tibet) Plateau (4): Quaternary Glacial Geology (in Chinese). Beijing: Geology Press. 131−136
Liang F, Cheng G. 1984. Polygon-veins along the Qinghai-Xizang Highway (in Chinese). J Glaciol Geocryol, 6: 51–60
Liu J, Yu G, Chen X. 2002. Palaeoclimate simulation of 21 ka for the Tibetan Plateau and eastern Asia. Clim Dyn, 19: 575–583
Luo D L, Jin H J, Jin R, Yang X G, Lü L Z. 2014. Spatiotemporal variations of climate warming in northern Northeast China as indicated by freezing and thawing indices. Quat Int, 349: 187–195
Ma H. 1996. Studies on terraces of the Chaidam basin, and Huangshui and Huanghe (Yellow) rivers. Doctoral Dissertation (in Chinese). Lanzhou: Lanzhou University. 32−33
Mark B G, Harrison S P, Spessa A, New M, Evans D J A, Helmens K F. 2005. Tropical snowline changes at the last glacial maximum: A global assessment. Quat Int, 138-139: 168–201
Murton J B, Kolstrup E. 2003. Ice-wedge casts as indicators of paleotemperatures: Precise proxy or wishful thinking? Prog Phys Geogr, 27: 155–170
Owen L A, England J. 1998. Observations on rock glaciers in the Himalayas and Karakoram Mountains of northern Pakistan and India. Geomorphology, 26: 199–213
Owen L A, Finkel R C, Haizhou M, Spencer J Q, Derbyshire E, Barnard P L, Caffee M W. 2003. Timing and style of Late Quaternary glaciation in northeastern Tibet. Geo Soc Am Bull, 115: 1356–1364
Owen L A, Finkel R C, Ma H Z, Barnard P L. 2006. Late Quaternary landscape evolution in the Kunlun Mountains and Qaidam Basin, Northern Tibet: A framework for examining the links between glaciation, lake level changes and alluvial fan formation. Quat Int, 73: 154–155
Pan B, Chen F. 1997. Permafrost evolution in the northeastern Qinghai-Tibetan Plateau during the last 150000 years (in Chinese). J Glaciol Geocryol, 19: 124−132
Qi B, Hu D, Zhao X, Zhang X, Zhang Y, Yang X, Zhao Z, Gao X. 2014. Fossil sand wedges in the northern shore of Qinghai Lake: Discovery and paleoclimatic implications (in Chinese). J Glaciol Geocryol, 36: 1412−1419
Qiu G, Cheng G. 1995. Permafrost in China: Past and present (in Chinese). Quat Sci, 15: 13−22
Qiu S. 1985. Basic features of natural environments in Northeast China Plain during the Pleistocene. In: Collection of Papers presented in the Conference on Quaternary Glacial and Periglacial Landforms in China (in Chinese). Beijing: Science Press. 208−211
Ran Y H, Li X, Cheng G D, Zhang T J, Jin H J. 2012. Distribution of permafrost in China: An overview of existing permafrost maps. Permafrost Periglacial Process, 23: 322–333
Romanovskii N N. 1977. Formation of Polygonal-Wedge Structures. Novosibirsk: Science Press. 70–85
Schmid M O, Baral P, Gruber S, Shahi S, Shrestha T, Stumm D, Wester P. 2015. Assessment of permafrost distribution maps in the Hindu Kush Himalayan region using rock glaciers mapped in Google Earth. Cryosphere, 9: 2089–2099
Shen C, Tang L, Wang S. 1996. Vegetation and climate during the last 250000 years in Zoigê region (in Chinese). Acta Micropalaeontol Sin, 13: 401−406
Shi Y. 1998. Evolution of the cryosphere in the Tibetan Plateau, China and its relationship with the global change in the Mid Quaternary (in Chinese). J Glaciol Geocryol, 20: 197−208
Shi Y. 2006. Quaternary Glaciers in China and Environmental Changes (in Chinese). Beijing: Science Press. 134−138
Shi Y. 2011. New Theories on Quaternary Glaciation (in Chinese). Shanghai: Shanghai Science Outreach Press. 130−135
Shi Y, Zheng B, Li S. 1990. Last glaciation and the maximum glaciation in Qinghai-Xizang Plateau (in Chinese). J Glaciol Geocryol, 12: 1−16
Shi Y, Kong Z, Wang S, Tang L, Wang F, Yao T, Zhao X, Zhang P, Shi S. 1992. Basic features of Climate and Environment in China during the Holocene Megathermal Period. In: Shi Y, Kong Z, eds. Climate and Environment in China during the Holocene Megathermal Period (in Chinese). Beijing: Science Press. 1−18
Shi Y, Zheng B, Li S, Ye B. 1995. Studies on altitude and climatic environment in the middle and east parts of Tibetan Plateau during Quaternary maximum glaciation (in Chinese). J Glaciol Geocryol, 17: 99−112
Shi Y, Zheng B, Yao T. 1997. Glaciers and environments during the last glacial maximum (LGM) on the Tibetan Plateau (in Chinese). J Glaciol Geocryol, 19: 97−113
Shi Y, Zheng B, Su Z. 2000. Quaternary glaciations, glaciation periods, and interglacial cycles and environmental changes. In: Shi Y, ed. Glaciers and Environment in China (in Chinese). Beijing: Science Press. 320−355
Song H, Xia Y. 1990. Pingo scars and peatlands on the Sanjiang Plain. In: Formation and Evolution of Natural Environment in the NE China Plain, China (in Chinese). Harbin: Harbin Cartography Press. 209−216
Stroeven A P, Hättestrand C, Heyman J, Harbor J, Li Y K, Zhou L P, Caffee M W, Alexanderson H, Kleman J, Ma H Z, Liu G N. 2009. Landscape analysis of the Huang He headwaters, NE Tibetan Plateau—Patterns of glacial and fluvial erosion. Geomorphology, 103: 212–226
Sun G. 1998. Marshes and Peat in the Hengduan Mountains (in Chinese). Beijing: Science Press. 220−224
Sun J, Wang S, Wang Y, Zhou Y, Lin Z, Zhang Q, Chen S. 1985. Paleoenvironment in Northeast China during the Last Glaciations (in Chinese). Quat Sci, 6: 82−89
Tang L, Shen C. 1996. Progress in the study of vegetation and climate change since Pliocene in the Qinghai-Xizang Plateau (in Chinese). Adv Earth Sci, 11: 198−203
Tang L, Shen C, Kong Z, Wang F, Liu K. 1998. Pollen evidence of climate during the Last Glaciation Maximum in eastern Tibetan Plateau (in Chinese). J Glaciol Geocryol, 20: 42−44
Tian Z. 1981. A study about the traces of Quaternary glaciations of Mount Taibaishan, Shaanxi Province (in Chinese). J Northwest Univ, (3): 67−69
Tong B. 1993. Ice wedges in Northeast China (in Chinese). J Glaciol Geocryol, 15: 41−46
Vandenberghe J. 1992. Cryoturbations: A sediment structural analysis. Permafrost Periglacial Process, 3: 343–351
Vandenberghe J, Pissart A. 1993. Permafrost changes in Europe during the Last Glacial. Permafrost Periglacial Process, 4: 121–135
Vandenberghe J, Cui Z J, Zhao L, Zhang W. 2004. Thermal-contraction-crack networks as evidence for late-Pleistocene permafrost in Inner Mongolia, China. Permafrost Periglacial Process, 15: 21–29
Vandenberghe J, Wang X, Vandenberghe D. 2016. Very large cryoturbation structures of Last Permafrost Maximum age at the foot of the Qilian Mountains (NE Tibet Plateau, China). Permafrost Periglacial Process, 27: 138–143
Wang P X, Sun J J. 1994. Last glacial maximum in China: Comparison between land and sea. Catena, 23: 341–353
Wang S. 1989. Formation and evolution of permafrost on the Qinghai-Xizang Plateau since the Late Pleistocene (in Chinese). J Glaciol Geocryol, 11: 67−75
Wang S, Bian C. 1993. The involutions and their palaeoclimatic significance in the Nachitai region along the Qinghai-Xizang Highway (in Chinese). Geogr Res, 132: 94−100
Wang X Y, Vandenberghe D, Yi S W, Vandenberghe J, Lu H Y, Van B R, Van H P. 2013. Late Quaternary paleoclimatic and geomorphological evolution at the interface between the Menyuan basin and the Qilian Mountains, northeastern Tibetan Plateau. Quat Res, 80: 534–544

Wei G B, Hu S M, Yu K F, Hou Y M, Li X, Jin C Z, Wang Y, Zhao J X, Wang W H. 2010. New materials of the steppe mammoth, *Mammuthus trogontherii*, with discussion on the origin and evolutionary patterns of mammoths. Sci China Earth Sci, 53: 956–963

Xing Z, Ou R. 1983. Study on the permafrost table from the changes in contents of salt and clay minerals. In: Lanzhou Institute of Glaciology and Geocryology, Chinese Academy of Sciences, ed. Proceedings of the 2nd Chinese Conference on Geocryology (in Chinese). Lanzhou: Gansu People's Press. 15−164

Xu S, Pan B. 1990. Periglacial wedge structures on eastern Qinghai Plateau and their formation environments. In: Lanzhou Institute of Glaciology and Geocryology, Chinese Academy of Sciences, ed. Proceedings of the 4th Chinese Conference on Glaciolology and Geocryology (Geocryology Volume) (in Chinese). Beijing: Science Press, 17−24

Xu S, Zhang W, Xu D, Xu Q, Shi S. 1984. Discussion on the periglacial development in the northeast margin regional of Qinghai-Xizang Plateau (in Chinese). J Glaciol Geocryol, 6: 15−24

Xu Z W, Lu H Y, Yi S W, Vandenberghe J, Mason J A, Zhou Y L, Wang X Y. 2015. Climate-driven changes to dune activity during the Last Glacial Maximum and deglaciation in the Mu Us dune field, north-central China. Earth Planet Sci Lett, 427: 149–159

Yang S Z, Jin H J. 2010. δ^{18}O and δD records of inactive ice wedge in Yitulihe, Northeastern China and their paleoclimatic implications. Sci China Earth Sci, 54: 119–126

Yang S Z, Cao X, Jin H J. 2015. Validation of ice-wedge isotopes at Yituli'he, northeastern China as climate proxy. Boreas, 44: 502–510

Yang X, Du S, Zhang F. 2006. Evolution of palaeoclimate in Hulunbeir Plateau since the Late Pleistocene (in Chinese). J Nat Disast, 15: 157−159

Yang Y, Wang F. 1983. Pleistocene Glaciations and paleoclimate in Xizang (Tibet). In: Quaternary Geology in Xizang (Tibet) (in Chinese). Beijing: Science Press. 91−99

Yao T, Shi Y. 1992. Changes of Holocene Climate recorded in the Dunde Ice-cores in the Qilian Mountains. In: Shi Y, ed. Clim Environ in China during the Holocene Megathermal Period (in Chinese). Beijing: Ocean Press. 206−211

Yu K, Lu H, Lehmkuhl F, Nottebaum V. 2013. A preliminary quantitative paleoclimate reconstruction of the dune fields of North China during the Last Glacial Maximum and Holocene Optimum (in Chinese). Quat Sci, 33: 293−302

Zhang H. 2009. A review of the study of environmental changes and extinction of the *Mamuthus-Colelodonta* Fauna during the Middle-Late Pleistocene in NE China (in Chinese). Adv Earth Sci, 24: 49−60

Zhang W. 1983. Charcteristics of sand wedges along the Qinghai-Xizang (Tibet) Highway and their formation time. In: Lanzhou Institute of Glaciology and Cryopedology (Geocryology), Chinese Academy of Sciences, ed. Proceedings of the 2nd Chinese Conference on Geocryology (in Chinese). Lanzhou: Gansu People's Press. 52−57

Zhao L, Jin H J, Li C C, Cui Z J, Chang X L, Marchenko S S, Vandenberghe J, Zhang T J, Luo D L, Guo D X, Liu G N, Yi C L. 2013. The extent of permafrost in China during the local Last Glacial Maximum (LLGM). Boreas, 43: 688–698

Zheng B. 1990. The glacier, environment and its changes since the Last Glaciation in West China (in Chinese). Quat Sci, 10: 101−110

Zheng Z, Yuan B Y, Petit-Maire N N. 1998. Paleoenvironments in China during the Last Glaciation Maximum and the Holocene Optimum. Episodes, 21: 152–158

Zhou T. 2007. Evolution of permafrost boundaries in China since the Penultimate Glaciation. Dissertation for Master Degree (in Chinese). Lanzhou: Lanzhou Unviersity. 1–59

Zhou T, Pan B, Liu X, Su H, Hu Z. 2008. The discovery of ice-wedge casts in Erdos: Rebuilding the permafrost boundary during the Penultimate Glaciation in China (in Chinese). Quat Sci, 30: 108−112

Zhou Y. 1965. Permafrost along the Qinghai-Xizang (Tibet) Highway. In: Collective Papers on Permafrost Expeditions along the Qinghai-Xizang (Tibet) Highway (in Chinese). Beijing: Science Press. 1−10

Zhou Y W, Qiu G Q, Guo D X. 1991. Quaternary permafrost in China. Quat Sci Rev, 10: 511–517

Zhou Y, Qiu G, Cheng G, Guo D, Li S. 2000. Geocryology in China (in Chinese). Beijing: Science Press. 366−388

Zhu K. 1972. Preliminary discussion on climate evolution in China during the last 5000 years (in Chinese). Acta Archaeol Sin, (1): 15−38

(Responsible editor: Huayu LU)